REPORT

Missense Mutations of the Pro65 Residue of PCGF2 Cause a Recognizable Syndrome Associated with Craniofacial, Neurological, Cardiovascular, and Skeletal Features

Peter D. Turnpenny,[1,28,*] Michael J. Wright,[2] Melissa Sloman,[3] Richard Caswell,[4] Anthony J. van Essen,[5,29] Erica Gerkes,[5] Rolph Pfundt,[6] Susan M. White,[7,8] Nava Shaul-Lotan,[9] Lori Carpenter,[10] G. Bradley Schaefer,[11] Alan Fryer,[12] A. Micheil Innes,[13] Kirsten P. Forbes,[14] Wendy K. Chung,[15] Heather McLaughlin,[16] Lindsay B. Henderson,[16] Amy E. Roberts,[17] Karen E. Heath,[18,19] Beatriz Paumard-Hernández,[18,19] Blanca Gener,[19,20] the DDD study,[21] Katherine A. Fawcett,[22,27] Romana Gjergja-Juraški,[23] Daniela T. Pilz,[24] and Andrew E. Fry[25,26,28,*]

PCGF2 encodes the polycomb group ring finger 2 protein, a transcriptional repressor involved in cell proliferation, differentiation, and embryogenesis. PCGF2 is a component of the polycomb repressive complex 1 (PRC1), a multiprotein complex which controls gene silencing through histone modification and chromatin remodelling. We report the phenotypic characterization of 13 patients (11 unrelated individuals and a pair of monozygotic twins) with missense mutations in *PCGF2*. All the mutations affected the same highly conserved proline in PCGF2 and were *de novo*, excepting maternal mosaicism in one. The patients demonstrated a recognizable facial gestalt, intellectual disability, feeding problems, impaired growth, and a range of brain, cardiovascular, and skeletal abnormalities. Computer structural modeling suggests the substitutions alter an N-terminal loop of PCGF2 critical for histone biding. Mutant PCGF2 may have dominant-negative effects, sequestering PRC1 components into complexes that lack the ability to interact efficiently with histones. These findings demonstrate the important role of PCGF2 in human development and confirm that heterozygous substitutions of the Pro65 residue of PCGF2 cause a recognizable syndrome characterized by distinctive craniofacial, neurological, cardiovascular, and skeletal features.

PCGF2 [MIM 600346] encodes the polycomb group ring finger 2 protein (PCGF2, *aka* MEL18). The PCGF2 protein contains an N-terminal RING finger motif and is similar in structure to other polycomb-group (PcG) proteins.[1] PCGF2 has been implicated in cell proliferation,[2] X inactivation,[3] regulation of homeobox genes during embryogenesis,[4] mesoderm differentiation,[5] hemopoiesis,[6] tumor suppression,[7,8] and angiogenesis.[9,10] PCGF2 is widely expressed in human tissues.[1,11] It binds to a specific DNA sequence (5′-GACTNGACT-3′) in the promoter regions of target genes.[7] PCGF2 is a component of a multiprotein complex called the polycomb repressive complex 1 (PRC1), an essential regulator, via histone modification and chromatin remodeling, of transcription in embryonic and adult stem cells.[12,13] The core of mammalian PRC1 typically contains an E3 ubiquitin ligase (RING1A [MIM 602045] or RING1B [MIM 608985]),[3,14] that ubiquitinates histone H2A at lysine 119, along with a PCGF protein (PCGF1-6),[15] which regulates the enzyme activity of the complex. PRC1 complexes often include other PcG components (e.g., polyhomeotic homolog or chromobox homolog proteins),

[1]Peninsula Clinical Genetics, Royal Devon and Exeter NHS Foundation Trust, Exeter EX1 2ED, UK; [2]Northern Genetics Service, Newcastle-upon-Tyne Hospitals NHS Foundation Trust, Newcastle NE1 3BZ, UK; [3]Department of Molecular Genetics, Royal Devon and Exeter NHS Foundation Trust, Exeter EX2 5DW, UK; [4]Institute of Biomedical and Clinical Science, University of Exeter Medical School, Exeter EX1 2LU, UK; [5]Department of Genetics, University of Groningen, University Medical Center Groningen, 9700 RB Groningen, the Netherlands; [6]Human Genetics, Radboud University Nijmegen Medical Centre, 6525 GA Nijmegen, the Netherlands; [7]Victorian Clinical Genetics Services, Murdoch Children's Research Institute, Parkville, Victoria 3052, Australia; [8]Department of Paediatrics, University of Melbourne, Parkville, Victoria 3052, Australia; [9]Clinical Genetics, Hadassah-Hebrew University Medical Center, Ein Kerem, Jerusalem 91120, Israel; [10]Saint Francis Genetics, Tulsa, Oklahoma 74136, USA; [11]University of Arkansas for Medical Sciences, Little Rock, Arkansas 72205, USA; [12]Cheshire and Merseyside Clinical Genetic Service, Liverpool Women's NHS Foundation Trust, Liverpool L8 7SS, UK; [13]Department of Medical Genetics and Alberta Children's Hospital Research Institute, Cumming School of Medicine, University of Calgary, Calgary, Alberta T3B 6A8, Canada; [14]Department of Neuroradiology, Queen Elizabeth University Hospital, Glasgow G51 4TF, UK; [15]Departments of Pediatrics and Medicine, Columbia University, New York, NY 10032, USA; [16]GeneDx, Gaithersburg, Maryland 20877, USA; [17]Cardiovascular Genetics, Department of Cardiology and Division of Genetics, Department of Medicine, Boston Children's Hospital, Boston, Massachusetts 02115, USA; [18]Institute of Medical & Molecular Genetics (INGEMM) and Skeletal Dysplasia Multidisciplinary Unit (UMDE), Hospital Universitario la Paz, Universidad Autónoma de Madrid, IdiPAZ, 28046 Madrid, Spain; [19]Centro de Investigación Biomédica en Red Enfermedades Raras (CIBERER), Instituto de Salud Carlos III (ISCII), 28029 Madrid, Spain; [20]Department of Genetics, Cruces University Hospital, Biocruces Health Research Institute, 48903 Barakaldo, Bizkaia, Spain; [21]Wellcome Trust Sanger Institute, Hinxton, Cambridge CB10 1SA, UK; [22]MRC Computational Genomics Analysis and Training Programme (CGAT), MRC Centre for Computational Biology, MRC Weatherall Institute of Molecular Medicine, John Radcliffe Hospital, Headington, Oxford OX3 9DS, UK; [23]Medical School of Osijek, Josip Juraj Strossmayer University, Neuropediatric Unit, Children's Hospital Srebrnjak, CRO-10000 Zagreb, Croatia; [24]West of Scotland Genetic Services, Queen Elizabeth University Hospital, Glasgow G51 4TF, UK; [25]Institute of Medical Genetics, University Hospital of Wales, Cardiff CF14 4XW, UK; [26]Division of Cancer and Genetics, School of Medicine, Cardiff University, Cardiff CF14 4XN, UK
[27]Present address: Department of Health Sciences, University of Leicester, George Davies Centre, University Road, Leicester LE1 7RH, UK
[28]These authors contributed equally to this work
[29]Deceased
*Correspondence: peter.turnpenny@nhs.net (P.D.T.), fryae@cardiff.ac.uk (A.E.F.)
https://doi.org/10.1016/j.ajhg.2018.09.012.

which guide recruitment of PRC1 to the chromatin.[12] The variable composition of PRC1 allows the complex to modulate function depending on cell type and developmental stage. A range of other proteins involved in histone H2A ubiquitination have been linked to neurodevelopmental disorders.[16] These include proteins involved in both adding[17–19] and removing[20–22] ubiquitin from H2A. Here, we report that mutations in *PCGF2* cause a recognizable developmental disorder.

Individuals 1 and 2 underwent exome sequencing as part of the Deciphering Developmental Disorders (DDD) study.[23] Both individuals had the same *de novo* missense mutation in *PCGF2*, c.194C>T, p.(Pro65Leu), and strikingly similar facial appearances. Identification of additional subjects with *PCGF2* variants was achieved through contact with other institutions and via GeneMatcher.[24] Thus, nine further unrelated individuals and a pair of monozygotic twin sisters with missense mutations in *PCGF2* were ascertained. The unrelated individuals all had the same mutation, c.194C>T, p.(Pro65Leu). The twin sisters (individuals 3 and 4) had a different mutation at the same residue, c.193C>T, p.(Pro65Ser). All mutations were *de novo*, apart from individual 11 whose asymptomatic mother was found to be mosaic (21% in blood DNA). Most mutations were identified by trio exome sequencing. Individual 6 was ascertained based on clinical features and the diagnosis confirmed by targeted Sanger sequencing.

To delineate the phenotypic spectrum associated with PCGF2 mutations we collected detailed clinical information. Consent for publication of photographs was sought from the individuals' parents or legal guardians (Individual 13's parents did grant use of non-facial photographs - they are in Figure S2). Individuals who had evaluation or analysis beyond routine clinical care were part of research studies approved by either the Cambridge South Research Ethics Committee (10/H0305/83) or the Research Ethics Committee for Wales (09/MRE09/51). Detailed case reports for all the subjects are given in the Supplemental Note. Detailed molecular and clinical features for each individual are included in Table S1. Coding and protein positions for PCGF2 are based on GenBank accession codes NM_007144.2 (ENST00000360797.2) and NP_009075.1, respectively.

The 13 subjects (7 females and 6 males) ranged in age from 2 to 21 years. The individuals all had similar distinctive facial features, intellectual disability, and impaired growth (Table S1). Clinical images from 12 of the subjects are shown in Figures 1, S1 and S2. Consistent facial features included a broad forehead with frontal bossing (13/13); sparse, slow growing hair, particularly in the frontal and temporal regions (12/12); periorbital fullness (12/12); and malar hypoplasia (12/12). The subjects' ears were dysplastic (12/12), typically with a satyr configuration, and often small and low set. Mild facial hypotonia was common. This impaired articulation of speech and led to an open mouth posture and drooling (3/13). Patients often had short palpebral fissures (11/12) and/or oral aperture (7/12). A prominent nasal tip (10/13) and mandibular progrnathism (7/13) were common in older individuals. The combination of large forehead, prominent jaw and open mouth results in the face often appearing long (7/12). The InterFace software package[25] was used to generate a composite average face (Figure S2).

The intellectual disability and/or developmental delay in the subjects ranged from mild to severe. Most individuals had difficulties with verbal communication. Three had absent speech at the time of assessment (at 21 years, 9 years, and 30 months of age). Muscular hypotonia (9/13) and conductive hearing impairment (7/13) were common. Only two subjects had a history of confirmed seizures. MRI brain scans for eight individuals were available for review (Figure 2). Mild enlargement of the lateral ventricles was common. Polymicrogyria, a malformation of cortical development, was noted in four individuals (bilateral extensive polymicrogyria in the twins, and bilateral perisylvian polymicrogyria in individuals 6 and 12). An irregular gyral pattern was reported in individual 9 but the MRI was not available for review. Patchy to confluent white matter changes were present in all reviewed scans, most prominently around the atria of the lateral ventricles. The white matter changes varied in severity and were most marked in the individuals with polymicrogyria. In some areas the abnormal white matter had the appearance of prominent perivascular spaces. Individual 1 reportedly had a thin corpus callosum. Individual 9 was reported to have mild cerebellar vermis hypoplasia. MR angiography was performed in three individuals. This showed a variable degree of tortuosity and ectasia of the intra- and extracranial blood vessels. Tortuous retinal vessels were reported in individual 7.

Intrauterine growth restriction was noted during three pregnancies (borderline in one more). All the subjects had a birth weight below the mean for gestational age. Weight during childhood remained low, compounded by feeding difficulties (9/13) and/or gastresophageal reflux (6/13). The feeding problems and reflux improved slowly with age. Constipation was also common (8/12), sometimes severe. Height during childhood was generally low for age although three subjects had heights just above the mean. The effects on head size were variable. Individual 1, the oldest and most intellectually impaired individual in the group, had a relatively large head size from early childhood, originally attributed to arrested hydrocephalus (occipitofrontal circumference [OFC] +1.8 SD, height and weight 1–2 SD below the mean). Relative macrocephaly was noted in two other individuals. In contrast, four individuals had small heads (OFC < -2 SD). Eleven subjects had cardiac abnormalities. Findings included patent ductus arteriosus (PDA) (5/13), atrial septal defect (3/13), and dilatation of the ascending aorta (5/13). Individual 5 had a PDA and prolapse of both mitral and tricuspid valves with some regurgitation. Individual 10 had aortic dilatation and an episode of supraventricular

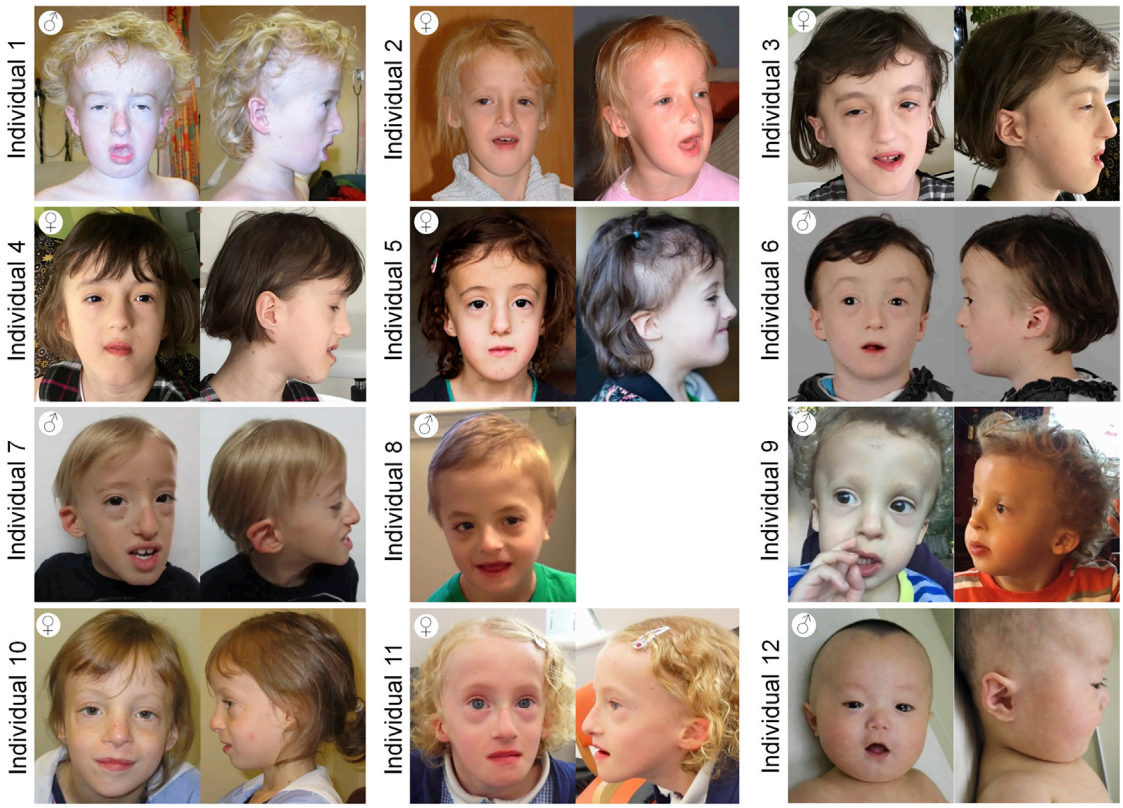

Figure 1. Facial Features of Individuals with *PCGF2* Mutations
Each individual is noted with the corresponding number used throughout the manuscript. Included on the top left of each cluster is the sex. Ages are: individual 1, 12 years; individual 2, 8.5 years; individual 3, 8 years; individual 4, 8 years; individual 5, 7 years (left), 4 years (right); individual 6, 9 years; individual 7, 7 years; individual 8, 6 years; individual 9, 2 years (left), 3 years (right); individual 10, 9 years; individual 11, 8 years; individual 12, 3 months. Consistent facial features include a broad forehead, long face, malar hypoplasia, small mouth, small palpebral fissures, periorbital fullness, prominent nose (particularly in older indiduals), and dysplastic, low-set ears.

tachycardia. Individual 1 was found to have a severely dilated aortic root at the age of 21 years (diameter 4.7 cm at the sinus of valsalva, Z score > 7). No arterial aneurysms or dissections were reported in the subjects. Skeletal anomalies were observed in several individuals. These included hypoplasia of the L1 vertebra (individual 1), small T3 vertebral body (individual 5), and a truncated sacrum (individual 6). Kyphosis and/or scoliosis (6/13), pectus deformities (3/13), and minor digital anomalies (4/13) were also found. Individual 1 had a skeletal survey at age 2.5 years, which revealed delayed epiphyseal ossification, particularly of the carpal bones, and pseudoepiphyses of many metacarpal bones. Two cases (individuals 2 and 4) had a small diaphragmatic hernia of the Morgagni type.

The identified mutations all affected the Pro65 residue of PCGF2. This residue is located just after the N-terminal RING finger motif and is highly conserved across species and other human PCGF proteins (Figures 3A and 3B). No variants have been reported at this position in the gnomAD database in PCGF2 or at the equivalent proline in other human PCGF proteins. Both mutations were predicted to be deleterious by a majority of *in silico* prediction programs (Table S1). To explore the effects of Pro65 mutations, we modeled the structure of the N-terminal of PCGF2 (amino acids 5-101) based on solved crystal structures for its homolog, BMI1 (PCGF4) [MIM 164831]. Two templates were used, PDB 2h0d (BMI1 bound to RING1B)[26] and PDB 4r8p (BMI1-PRC1 complex bound to nucleosome),[27] with essentially identical results. Pro65 is situated at the junction between an extended loop region and a short α-helix (Figure 3C). The presence of proline at this position is likely to maintain the transition from loop to helix. Furthermore, given the rotational constraint imposed by proline's ring structure, this residue is likely to provide the loop region with a degree of structural rigidity.[28] Thermodynamic analysis of the 2h0d-based PCGF2 model using FoldX showed the Pro65 variants resulted in changes to thermodynamic stability (ΔΔG) of +8.6 kcal/mol and +3.9 kcal/mol for p.Pro65Leu and p.Pro65Ser respectively; ΔΔG values values > 3 kcal/mol are generally regarded as destabilizing.[29] Intriguingly, the loop region next to Pro65 contains two basic residues, Lys62 and Arg64, which form a basic patch on BMI1 and the predicted surface of PCGF2 (Figures 3D and 3E). PRC1 complexes containing PCGF2 (or BMI1) have low intrinsic ubiquitin ligase activity compared to complexes containing other PCGF proteins.[30] This is compensated

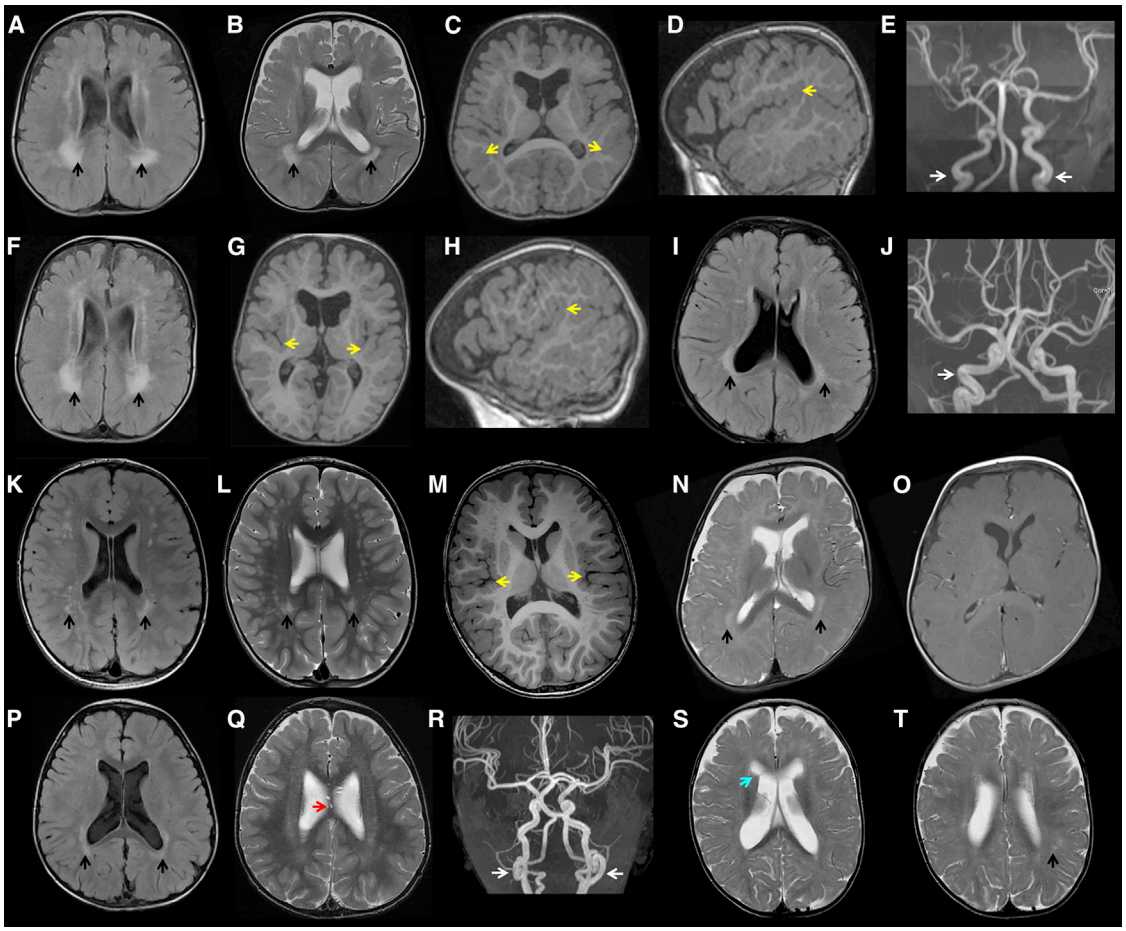

Figure 2. MRI Brain Abnormalities in Individuals with *PCGF2* Mutations
(A–E) Axial (FLAIR, T2 and T1), sagittal (T1), and MRA images from individual 3 at age 21 months.
(F–H) Axial (FLAIR and T1) and sagittal (T1) images from individual 4 at age 21 months.
(I and J) Axial FLAIR and MRA images from individual 5 at age 3 years and 3 months.
(K–M) Axial (FLAIR, T2 and T1) images from individual 6 at age 5 years.
(N and O) Axial (T2 and T1) images from individual 7 at age 10 months.
(P–R) Axial (FLAIR and T2) and MRA images from individual 8 at age 37 months.
(S and T) Axial T2 images from individual 10 at age 13 months.
The images show patchy white matter hyperintensity in the T2 and FLAIR images (black arrows). The patches are scattered throughout the white matter but are consistently seen in the peri-atrial region. Other findings included enlargement of the lateral ventricles; increased anterior extra-axial fluid spaces (e.g., B, G, N, and S); bilateral polymicrogyria (yellow arrows, subtle in M); prominence of the perivascular spaces, including in the corpus callosum (red arrow, Q); coarctation of the frontal horns (blue arrow, S). MRA showed tortuosity (white arrows) of the internal carotid (E), (J), and vertebral (R) arteries.

for by an increased affinity for the nucleosomal substrate, leading to efficient histone ubiquitination. The increased affinity is dependent on residues Lys62 and Arg64, which interact with an acidic patch on the surface of histones 3 and 4 (Figure 3F). This raises the possibility that the interaction between PCGF2 and histones is disrupted by the structural perturbations caused by Pro65 substitutions.

The extreme clustering of disease-causing *de novo* missense mutations in *PCGF2* is highly statistically significant and similar to other genes with non-haploinsufficient disease mechanisms.[31] No truncating mutations were observed in our cohort. In contrast, several truncating *PCGF2* variants are listed by the gnomAD database. This argues against a simple haploinsufficiency mechanism. The probability of *PCGF2* being loss-of-function intolerant (pLI)[32] in the Exome Aggregation Consortium (ExAC) database is only 0.55. Furthermore, no interstitial deletions involving *PCGF2* are listed on the DECIPHER database. Loss of *PSc* (the homolog of *PCGF*) in *Drosophila melanogaster* leads to mis-expression of homeotic genes and defects in segmental determination.[33] Similarly, homzoygote *Pcgf2*-deficient mice exhibit disturbed Hox gene expression with posterior transformations of the axial skeleton and growth retardation.[4] However, heterozygous *Pcgf2*-deficient mice were normal, and no abnormalities of craniofacial structure or neurology were identified in the homozygotes. Our *in silico* structural modeling suggests substitution of Pro65 disrupts the interaction of PCGF2 with histones. This provides a plausible molecular mechanism for a dominant-negative effect. Mutant PCGF2 might

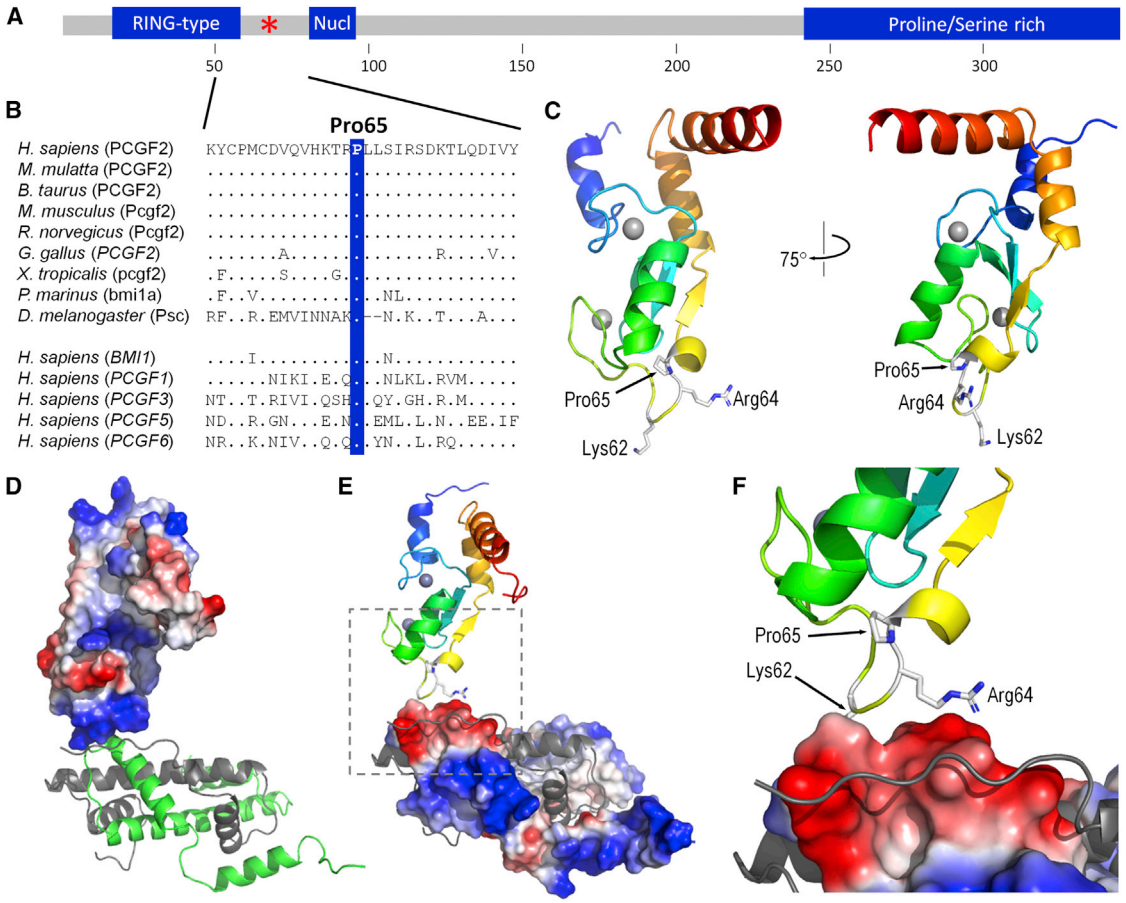

Figure 3. Localization of the PCGF2 Mutations

(A) Schematic domains of PCGF2. The domains and motifs of PCGF2 (UniprotKB: P35227) are illustrated. These include a RING-type Zinc finger (residues 18–57), nuclear localization signal (81–95) and Proline/Serine-rich domain (242–344). The location of the Pro65 residue is marked by the red asterisk. Residue number is indicated in the scale below the illustration.

(B) The PCGF2 mutations are located at the highly conserved Pro65 residue. ClustalW homology alignments for Human PCGF2 (residues 51-80) and a range of orthologs and paralogs. Orthologs include Human (NP_009075.1), Rhesus monkey (XP_001083817.1), Cow (NP_001137578.1), Mouse (NP_001156779.1), Rat (NP_001099306.1), Chicken (XP_003642857.1), Frog (NP_001025573.1), Lamprey (ENSPMAP00000007297.1), and Fruit fly (NP_523725.2). Paralogs include BMI1/PCGF4 (NP_005171.4), PCGF1 (NP_116062.2), PCGF3 (NP_006306.2), PCGF5 (NP_001243478.1), and PCGF6 (NP_001011663.1). Identical residues are indicated by dots. The blue bar highlights the position of the Pro65 residue.

(C) Structural model of human PCGF2 (residues 5-101, modeled on template 2h0d). Two views of the model are shown in ribbon format, colored from blue, N-terminal, to red, C-terminal, with side-chains shown for Pro65, Arg64, and Lys62. Grey spheres represent bound zinc ions; interaction with RING1B is primarily mediated via residues in helices 1 and 3 (blue and orange, respectively).

(D) The interaction between PCGF2 and histone H3/4 (modeled on template 4r8p). The predicted molecular surface of PCGF2 (left) is colored by electrostatic charge (blue, basic; red, acidic); histone chains from 4r8p are shown as green (H3.2) and gray (H4) ribbons, respectively; other chains of the complex have been omitted for clarity; note the basic patch of PCGF2 in contact with H3.2.

(E) As (D), but showing surface charge for H3.2, with PCGF2 shown as a ribbon colored from N-terminal, blue to C-terminal, red; note the acidic patch of H3.2 lying opposite the basic patch of PCGF2.

(F) As (E), but showing detail around the PCGF2/H3.2 interface; the regions shown are outlined by gray broken lines in part E; sidechains of PCGF2 Pro65, Arg64, and Lys62 (partially obscured) are shown in stick format.

retain the ability to sequester other PcG components into PRC1 complexes but, due to disruption of the loop structure around Lys62 and Arg64, mutant PRC1 complexes might lack the ability to interact efficiently with histones. Detailed functional experiments will be required to distinguish between these and other possible pathogenesic mechanisms at a molecular level.

PCGF2 regulates differentiation of the cardiac mesoderm, which might contribute to the cardiac anomalies seen.[5] Aortic dilation was found in five of the subjects (severe in individual 1, the young adult). We would therefore recommend that all *PCGF2* patients have periodic echocardiographic surveillance. The brain and vascular abnormalities seen in patients might be due to disturbed PI3K-AKT signaling, a critical pathway regulating growth, angiogenesis, and neural development. Loss of PCGF2 function leads to downregulation of PTEN [MIM 601728], promoting activation of AKT [MIM 164730], increased HIF-1α [MIM 603348] levels, and expression of vascular endothelial growth factor [MIM 192240].[10] In addition, PCGF2

binds directly to CCND2 [MIM 123833], a downstream effector of the PI3K-AKT pathway in developing neuroblasts.[34] Gain-of-function mutations in *CCND2* and other components of the PI3K-AKT pathway have been found to cause polymicrogyria, macrocephaly, and ventricular dilation.[35,36] Knockdown of PCGF2 has been shown to increase proliferative activity in cells overexpressing CCND2.[34] If Pro65 mutations reduce PCGF2's ability to inhibit CCND2, the increased CCND2 activity may predispose to polymicrogyria. The CCND2 binding site has been mapped to the C-terminal proline/serine-rich domain of PCGF2.[34] Therefore, mutation of the N-terminal Pro65 residue is unlikely to directly block binding of CCND2. The presence of vascular abnormalities (and the twin placental circulation of individuals 3 and 4) may be additional risk factors for the polymicrogyria.[37] The variable head size observed in subjects may reflect the conflicting effects of abnormal vasculature (impairing brain growth and causing the deep cerebral white matter changes) and altered signaling through the PI3K-AKT-CCND2 pathway (promoting brain growth and ventricular dilation). PCGF2 has tumor suppression activity and has been implicated in a range of tumor types.[7,38–40] To date, none of the subjects with PCGF2 Pro65 mutations has been diagnosed with malignancy.

In summary, we have reported 13 individuals with missense substitutions of the Pro65 residue of PCGF2. These individuals have a recognizable phenotype of developmental delay, intellectual disability, impaired growth, and characteristic facial features that include frontal bossing, sparse hair, malar hypoplasia, small palpebral fissures and oral stoma, and dysplastic "satyr" ears. Other common findings in the subjects included feeding problems, constipation, and a range of brain, cardiac, vascular, and skeletal malformations. Further work is required to define the precise pathogenic mechanism of *PCGF2* mutations; however, our modeling and the available genetic data suggests that PCGF2 Pro65 mutations have dominant-negative effects on PRC1 function, altering multiple signaling pathways and therefore resulting in the complex human phenotype.

Supplemental Data

Supplemental data include two figures, one table, and a Supplemental Note and can be found with this article online at https://doi.org/10.1016/j.ajhg.2018.09.012.

Acknowledgments

We thank the individuals and their families for their willingness to participate in this study. We are grateful to Caroline Wright (Exeter) for her comments on the manuscript and to Bert de Vries (Nijmegen), Orly Elpeleg (Jerusalem), and Megan Cho (GeneDx) for alerting us to new cases that would not otherwise have been part of this collaboration.

A.E.F. was supported by the Academy of Medical Sciences (grant: AMS-SGCL8-Fry). This work was also supported by the Wales Epilepsy Research Network and the Wales Gene Park. W.K.C. received support from the Simons Foundation and JPB Foundation. K.E.H. received support from MINECO (grants: SAF2015-66831-R, SAF2017-84646-R). The DDD study presents independent research commissioned by the Health Innovation Challenge Fund (grant number HICF-1009-003), a parallel funding partnership between the Wellcome Trust and the Department of Health, and the Wellcome Trust Sanger Institute (grant number WT098051). The views expressed in this publication are those of the author(s) and not necessarily those of the funding agencies.

Declaration of Interests

H.M. and L.B.H. are employees of GeneDx, Inc., a wholly owned subsidiary of OPKO Health, Inc. The other authors declare no competing interests.

Received: May 16, 2018
Accepted: September 22, 2018
Published: October 18, 2018

Web Resources

CADD, https://cadd.gs.washington.edu/
Deciphering Developmental Disorders, http://www.ddduk.org/
DECIPHER, https://decipher.sanger.ac.uk/
ExAC Browser, http://exac.broadinstitute.org/
FoldX, http://foldxsuite.crg.eu/
GenBank, https://www.ncbi.nlm.nih.gov/genbank/
GeneMatcher, https://genematcher.org/
gnomAD Browser, http://gnomad.broadinstitute.org/
InterFace Software Package, https://www.york.ac.uk/psychology/interface/
MutationTaster, http://www.mutationtaster.org/
OMIM, http://www.omim.org/
PolyPhen-2, http://genetics.bwh.harvard.edu/pph2/
RCSB Protein Data Bank, http://www.rcsb.org/pdb/home/home.do
SIFT, http://sift.bii.a-star.edu.sg/
SMART, http://www.smart.embl-heidelberg.de/
The Human Protein Atlas, http://www.proteinatlas.org/
SWISS-MODEL, http://swissmodel.expasy.org/
UCSC Genome Browser, https://genome.ucsc.edu
UniProt, http://www.uniprot.org/

References

1. Ishida, A., Asano, H., Hasegawa, M., Koseki, H., Ono, T., Yoshida, M.C., Taniguchi, M., and Kanno, M. (1993). Cloning and chromosome mapping of the human Mel-18 gene which encodes a DNA-binding protein with a new 'RING-finger' motif. Gene *129*, 249–255.
2. Guo, W.-J., Datta, S., Band, V., and Dimri, G.P. (2007). Mel-18, a polycomb group protein, regulates cell proliferation and senescence via transcriptional repression of Bmi-1 and c-Myc oncoproteins. Mol. Biol. Cell *18*, 536–546.
3. de Napoles, M., Mermoud, J.E., Wakao, R., Tang, Y.A., Endoh, M., Appanah, R., Nesterova, T.B., Silva, J., Otte, A.P., Vidal, M., et al. (2004). Polycomb group proteins Ring1A/B link ubiquitylation of histone H2A to heritable gene silencing and X inactivation. Dev. Cell *7*, 663–676.

4. Akasaka, T., Kanno, M., Balling, R., Mieza, M.A., Taniguchi, M., and Koseki, H. (1996). A role for mel-18, a Polycomb group-related vertebrate gene, during theanteroposterior specification of the axial skeleton. Development *122*, 1513–1522.
5. Morey, L., Santanach, A., Blanco, E., Aloia, L., Nora, E.P., Bruneau, B.G., and Di Croce, L. (2015). Polycomb Regulates Mesoderm Cell Fate-Specification in Embryonic Stem Cells through Activation and Repression Mechanisms. Cell Stem Cell *17*, 300–315.
6. Kajiume, T., Ninomiya, Y., Ishihara, H., Kanno, R., and Kanno, M. (2004). Polycomb group gene mel-18 modulates the self-renewal activity and cell cycle status of hematopoietic stem cells. Exp. Hematol. *32*, 571–578.
7. Kanno, M., Hasegawa, M., Ishida, A., Isono, K., and Taniguchi, M. (1995). mel-18, a Polycomb group-related mammalian gene, encodes a transcriptional negative regulator with tumor suppressive activity. EMBO J. *14*, 5672–5678.
8. Guo, W.-J., Zeng, M.-S., Yadav, A., Song, L.-B., Guo, B.-H., Band, V., and Dimri, G.P. (2007). Mel-18 acts as a tumor suppressor by repressing Bmi-1 expression and down-regulating Akt activity in breast cancer cells. Cancer Res. *67*, 5083–5089.
9. Jung, J.-H., Choi, H.-J., Maeng, Y.-S., Choi, J.-Y., Kim, M., Kwon, J.-Y., Park, Y.-W., Kim, Y.-M., Hwang, D., and Kwon, Y.-G. (2010). Mel-18, a mammalian Polycomb gene, regulates angiogenic gene expression of endothelial cells. Biochem. Biophys. Res. Commun. *400*, 523–530.
10. Park, J.H., Lee, J.Y., Shin, D.H., Jang, K.S., Kim, H.J., and Kong, G. (2011). Loss of Mel-18 induces tumor angiogenesis through enhancing the activity and expression of HIF-1α mediated by the PTEN/PI3K/Akt pathway. Oncogene *30*, 4578–4589.
11. Uhlén, M., Fagerberg, L., Hallström, B.M., Lindskog, C., Oksvold, P., Mardinoglu, A., Sivertsson, Å., Kampf, C., Sjöstedt, E., Asplund, A., et al. (2015). Proteomics. Tissue-based map of the human proteome. Science *347*, 1260419.
12. Aloia, L., Di Stefano, B., and Di Croce, L. (2013). Polycomb complexes in stem cells and embryonic development. Development *140*, 2525–2534.
13. Aranda, S., Mas, G., and Di Croce, L. (2015). Regulation of gene transcription by Polycomb proteins. Sci. Adv. *1*, e1500737.
14. Wang, H., Wang, L., Erdjument-Bromage, H., Vidal, M., Tempst, P., Jones, R.S., and Zhang, Y. (2004). Role of histone H2A ubiquitination in Polycomb silencing. Nature *431*, 873–878.
15. Gao, Z., Zhang, J., Bonasio, R., Strino, F., Sawai, A., Parisi, F., Kluger, Y., and Reinberg, D. (2012). PCGF homologs, CBX proteins, and RYBP define functionally distinct PRC1 family complexes. Mol. Cell *45*, 344–356.
16. Srivastava, A., McGrath, B., and Bielas, S.L. (2017). Histone H2A Monoubiquitination in Neurodevelopmental Disorders. Trends Genet. *33*, 566–578.
17. Awad, S., Al-Dosari, M.S., Al-Yacoub, N., Colak, D., Salih, M.A., Alkuraya, F.S., and Poizat, C. (2013). Mutation in PHC1 implicates chromatin remodeling in primary microcephaly pathogenesis. Hum. Mol. Genet. *22*, 2200–2213.
18. Beunders, G., Voorhoeve, E., Golzio, C., Pardo, L.M., Rosenfeld, J.A., Talkowski, M.E., Simonic, I., Lionel, A.C., Vergult, S., Pyatt, R.E., et al. (2013). Exonic deletions in AUTS2 cause a syndromic form of intellectual disability and suggest a critical role for the C terminus. Am. J. Hum. Genet. *92*, 210–220.
19. Pierce, S.B., Stewart, M.D., Gulsuner, S., Walsh, T., Dhall, A., McClellan, J.M., Klevit, R.E., and King, M.-C. (2018). De novo mutation in *RING1* with epigenetic effects on neurodevelopment. Proc. Natl. Acad. Sci. USA *115*, 1558–1563.
20. Hoischen, A., van Bon, B.W.M., Rodríguez-Santiago, B., Gilissen, C., Vissers, L.E.L.M., de Vries, P., Janssen, I., van Lier, B., Hastings, R., Smithson, S.F., et al. (2011). De novo nonsense mutations in ASXL1 cause Bohring-Opitz syndrome. Nat. Genet. *43*, 729–731.
21. Shashi, V., Pena, L.D.M., Kim, K., Burton, B., Hempel, M., Schoch, K., Walkiewicz, M., McLaughlin, H.M., Cho, M., Stong, N., et al.; Undiagnosed Diseases Network (2016). De Novo Truncating Variants in ASXL2 Are Associated with a Unique and Recognizable Clinical Phenotype. Am. J. Hum. Genet. *99*, 991–999.
22. Bainbridge, M.N., Hu, H., Muzny, D.M., Musante, L., Lupski, J.R., Graham, B.H., Chen, W., Gripp, K.W., Jenny, K., Wienker, T.F., et al. (2013). De novo truncating mutations in ASXL3 are associated with a novel clinical phenotype with similarities to Bohring-Opitz syndrome. Genome Med. *5*, 11.
23. Deciphering Developmental Disorders Study (2015). Large-scale discovery of novel genetic causes of developmental disorders. Nature *519*, 223–228.
24. Sobreira, N., Schiettecatte, F., Valle, D., and Hamosh, A. (2015). GeneMatcher: A Matching Tool for Connecting Investigators with an Interest in the Same Gene. Hum. Mutat. https://doi.org/10.1002/humu.22844.
25. Kramer, R.S.S., Jenkins, R., and Burton, A.M. (2017). InterFace: A software package for face image warping, averaging, and principal components analysis. Behav. Res. Methods *49*, 2002–2011.
26. Li, Z., Cao, R., Wang, M., Myers, M.P., Zhang, Y., and Xu, R.-M. (2006). Structure of a Bmi-1-Ring1B polycomb group ubiquitin ligase complex. J. Biol. Chem. *281*, 20643–20649.
27. McGinty, R.K., Henrici, R.C., and Tan, S. (2014). Crystal structure of the PRC1 ubiquitylation module bound to the nucleosome. Nature *514*, 591–596.
28. Jacob, J., Duclohier, H., and Cafiso, D.S. (1999). The role of proline and glycine in determining the backbone flexibility of a channel-forming peptide. Biophys. J. *76*, 1367–1376.
29. Tokuriki, N., and Tawfik, D.S. (2009). Stability effects of mutations and protein evolvability. Curr. Opin. Struct. Biol. *19*, 596–604.
30. Taherbhoy, A.M., Huang, O.W., and Cochran, A.G. (2015). BMI1-RING1B is an autoinhibited RING E3 ubiquitin ligase. Nat. Commun. *6*, 7621.
31. Lelieveld, S.H., Wiel, L., Venselaar, H., Pfundt, R., Vriend, G., Veltman, J.A., Brunner, H.G., Vissers, L.E.L.M., and Gilissen, C. (2017). Spatial Clustering of de Novo Missense Mutations Identifies Candidate Neurodevelopmental Disorder-Associated Genes. Am. J. Hum. Genet. *101*, 478–484.
32. Lek, M., Karczewski, K.J., Minikel, E.V., Samocha, K.E., Banks, E., Fennell, T., O'Donnell-Luria, A.H., Ware, J.S., Hill, A.J., Cummings, B.B., et al.; Exome Aggregation Consortium (2016). Analysis of protein-coding genetic variation in 60,706 humans. Nature *536*, 285–291.
33. Adler, P.N., Martin, E.C., Charlton, J., and Jones, K. (1991). Phenotypic consequences and genetic interactions of a null mutation in the Drosophila Posterior Sex Combs gene. Dev. Genet. *12*, 349–361.
34. Chun, T., Rho, S.B., Byun, H.-J., Lee, J.-Y., and Kong, G. (2005). The polycomb group gene product Mel-18 interacts with cyclin D2 and modulates its activity. FEBS Lett. *579*, 5275–5280.

35. Rivière, J.-B., Mirzaa, G.M., O'Roak, B.J., Beddaoui, M., Alcantara, D., Conway, R.L., St-Onge, J., Schwartzentruber, J.A., Gripp, K.W., Nikkel, S.M., et al.; Finding of Rare Disease Genes (FORGE) Canada Consortium (2012). De novo germline and postzygotic mutations in AKT3, PIK3R2 and PIK3CA cause a spectrum of related megalencephaly syndromes. Nat. Genet. *44*, 934–940.
36. Mirzaa, G., Parry, D.A., Fry, A.E., Giamanco, K.A., Schwartzentruber, J., Vanstone, M., Logan, C.V., Roberts, N., Johnson, C.A., Singh, S., et al.; FORGE Canada Consortium (2014). De novo CCND2 mutations leading to stabilization of cyclin D2 cause megalencephaly-polymicrogyria-polydactyly-hydrocephalus syndrome. Nat. Genet. *46*, 510–515.
37. Stutterd, C.A., and Leventer, R.J. (2014). Polymicrogyria: a common and heterogeneous malformation of cortical development. Am. J. Med. Genet. C. Semin. Med. Genet. *166C*, 227–239.
38. Lu, Y.-W., Li, J., and Guo, W.-J. (2010). Expression and clinicopathological significance of Mel-18 and Bmi-1 mRNA in gastric carcinoma. J. Exp. Clin. Cancer Res. *29*, 143.
39. Tao, J., Liu, Y.-L., Zhang, G., Ma, Y.-Y., Cui, B.-B., and Yang, Y.-M. (2014). Expression and clinicopathological significance of Mel-18 mRNA in colorectal cancer. Tumour Biol. *35*, 9619–9625.
40. Won, H.-Y., Lee, J.-Y., Shin, D.-H., Park, J.-H., Nam, J.-S., Kim, H.-C., and Kong, G. (2012). Loss of Mel-18 enhances breast cancer stem cell activity and tumorigenicity through activating Notch signaling mediated by the Wnt/TCF pathway. FASEB J. *26*, 5002–5013.